Noise resolution of RuO_2-based resistance thermometers

Piotr Ptak,[a] Andrzej Kolek, Zbigniew Zawislak, Adam W. Stadler, and Krzysztof Mleczko
Department of Electronics Fundamentals, Rzeszow University of Technology, W. Pola 2, 35-959 Rzeszow, Poland

(Received 23 February 2004; accepted 10 September 2004; published online 22 December 2004)

Low-frequency noise was measured for RuO_2-based thick film resistors at liquid helium temperatures down to 0.36 K. The $1/f$-type spectrum and squared voltage dependence of power spectral density observed at low voltages attribute the noise as coming from equilibrium resistance fluctuations. Measurements carried out at different temperatures show that the magnitude of noise intensity (index) increases significantly as temperature goes down. Due to this fact, the resolution of RuO_2 thermometers increases above the instrument resolution. The quantity which describes a sensor resolution is defined and calculated for RuO_2 thick film sensor. Some remarks on measurement strategy and sensor optimization are supplied. © *2005 American Institute of Physics*. [DOI: 10.1063/1.1834704]

I. INTRODUCTION

Ruthenium based thick film resistors (TFR) are widely used in modern electronics. This is due to their nice properties, such as the wide range of sheet resistances, low voltage nonlinearity, a great capacity to dissipate power, the long-term stability, low noise, and very small temperature coefficient of resistance. Figure 1 presents, for example, a dependence of resistance R on temperature T for one of TFR fabricated in our laboratory. Indeed, very weak $R(T)$ dependence is observed in the room temperature range. On the other hand, a very rapid increase of resistance is observed as $T \rightarrow 0$. This makes sensitivity $|dR/dT|$ very large in the lowest temperatures. Another well-known feature of these resistors in low temperatures is very low magnetoresistance. For both these reasons Ru-based TFR are often used as thermometers in the liquid helium temperature range.

Recently a significant increase of low-frequency noise in RuO_2+glass TFR was observed as the temperature was lowered below a few kelvins.[1] This fact rises the question of how the increase of this noise restricts the resolution of such types of thermometers. The motivation for the study whose results are presented here was to resolve this question.

II. SAMPLE PREPARATION

The resistors used in the experiment were fabricated from the laboratory-prepared resistive paste of known composition. This paste was a mixture of RuO_2 powder of average grains' size of 13.7–25 nm, glass frit, and organic solvent. The glass consisted of 65% PbO, 10% B_2O_3, 25% SiO_2 by weight. Pastes containing various volume fractions v of conducting component (RuO_2) were prepared, but in this study only the resistors V12 made of paste with $v=0.12$ were considered. They were screen-printed on alumina substrates (96% Al_2O_3), and after printing, the resistors were dried and fired in the flow tunnel furnace with suitable temperature profile (850 °C peak temperature for 10 min). Conducting pads made of gold pastes (Au) were printed and fired before the final printing and firing of resistive paste.

For the measurements, resistors were prepared as four-terminal specimens with two voltage contacts along one its side (Fig. 2). The resistive film of the resistor was about 12 μm thick, 1 mm wide, and 6 mm long. The distance between the voltage contacts was 2 mm. Such shape of the specimens enables four-point resistance measurements to be done and, what is more important, this shape makes it possible to identify the noise sources on the macroscopic level. It may happen that noises originate not only from the bulk of sensing materials but also from the contacts. Separate voltage and current electrodes enable the bulk and contact components of the total noise to be distinguished.[2–4]

There are at least several reasons why we have used in our experiments the resistors made in our laboratory, instead of commercially available sensors. First and the most important was already mentioned above. Commercial sensors, even if they are supplied in a four-wire arrangement, usually have current and voltage leads mounted on the same conducting pad as it is shown in Fig. 2(b). With such a wiring the noises generated in the bulk of resistive film and in the

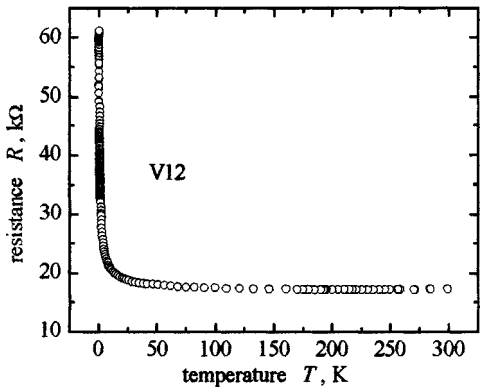

FIG. 1. Resistance vs temperature for a thick film resistor made from resistive ink, which contain $v=0.12$ of RuO_2 by volume.

[a]Electronic mail: pptak@prz.rzeszow.pl

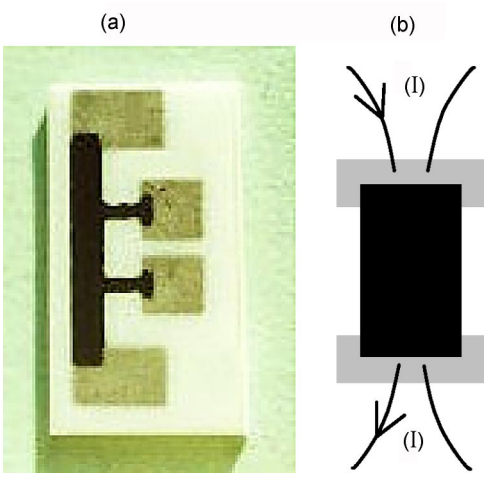

FIG. 2. (Color online) (a) Picture of a specimen used in the experiment. (b) Four-wire arrangement of leads in commercial sensors.

pad-film contacts adds up and cannot be separated. Another reason for making the sample the way we did, is that only in this case we know exactly their composition. They contain only RuO_2 and glass, both with known volume fractions. They do not contain any modifiers like, e.g., manganese, which can strongly influence the properties of RuO_2+glass composites.[5] This is important if one aims to identify the microscopic sources of the noise.

Before we shall proceed further, let us compare basic properties of our specimens with a sample low-temperature sensor available at the market. We have chosen Lake Shore sensor RX-202A, known for its good performance characteristics[6] (in fact, this sensor was used to monitor temperature in our cryostat). In Fig. 3 we compare sensitivity $|dR/dT|$ calculated for a pair of V12 samples (the reason why we have measured resistance of a pair of samples is explained in the next section) with that of RX-202A. As one can see, the sensitivity of samples V12 is almost an order of magnitude larger than that of RX-202A over a wide temperature range. In Figs. 4(a) and 4(b) the relative changes of apparent temperature versus magnetic field for RX-202A and for our samples V12 are compared. Although the data in Figs. 4(a) and 4(b) relate to different temperatures, it is clear that magnetic field induced errors for the samples V12 are smaller than that for the sensor RX-202A. The aim of this comparison is not to show that the V12 specimens are better than RX-202A because their nominal resistances differ by more than an order of magnitude, but to prove that the specimens we have used in our experiment fall into the same class of devices which are currently in practical use in low-temperature thermometry.

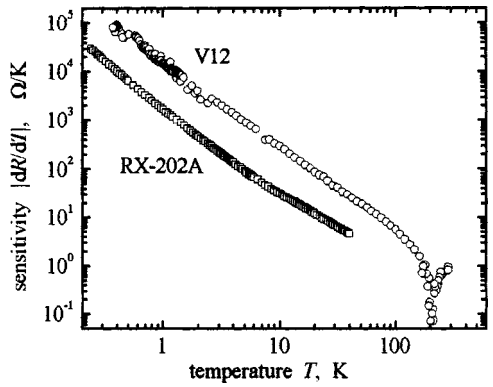

FIG. 3. Sensitivity $|dR/dT|$ vs temperature for a pair of our samples V12, and for Lake Shore sensor RX-202A (standard curve available at Ref. 6).

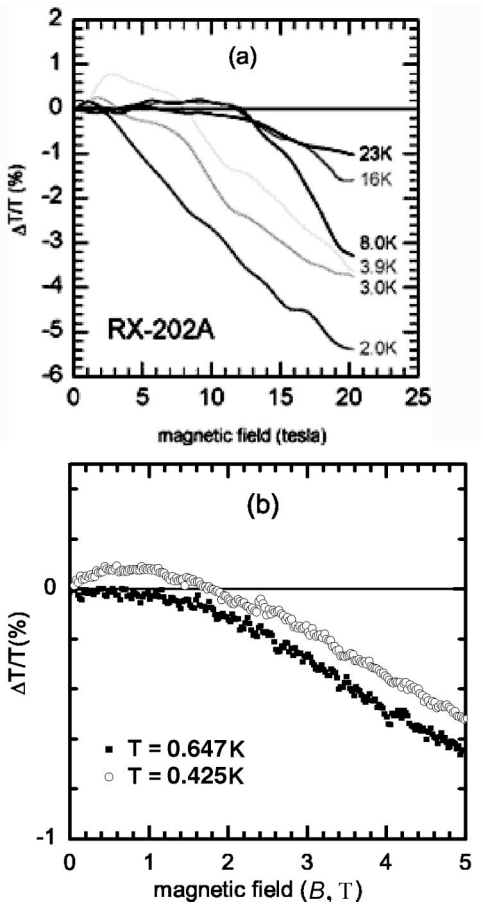

FIG. 4. Magnetic field induced errors, for (a) Lake Shore sensor model RX-202A and (b) samples V12, as a function of magnetic field at constant temperatures.

III. NOISE MEASUREMENTS

The measurements of low-frequency noise were performed with modulation-demodulation technique of Ref. 7. This technique enables to detect the noise at very low excitation. It is important at the liquid helium temperatures, when the self-heating of samples may occur. Figure 5 presents the

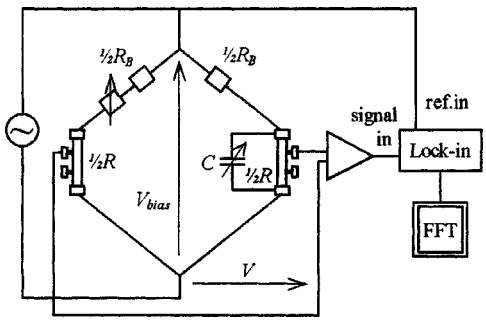

FIG. 5. Setup for ac noise measurements.

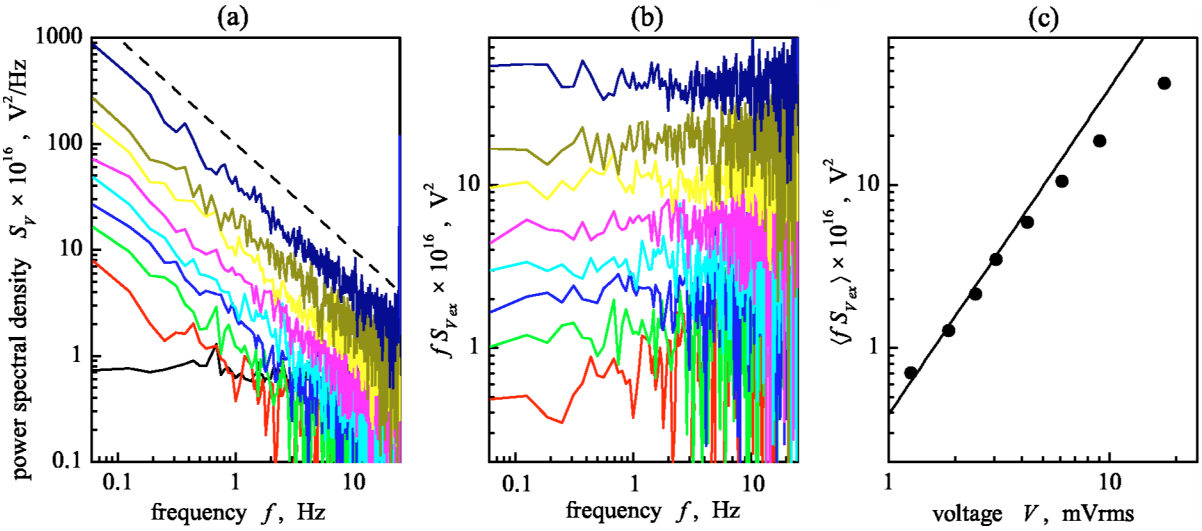

FIG. 6. (Color online) (a) Power spectral densities S_V of noise measured for a pair of V12 specimens at $T=0.45$ K for several ac voltages: $V=1.3$, 1.9, 2.5, 3.1, 4.3, 6.1, 9.1, 17.8 mVrms. Flat spectrum is the background noise $S_V=0$, measured with no bias. Dashed line has the slope −1 and shows "pure" $1/f$ noise. (b) Products of $S_{Vex}=S_V-S_{V=0}$ and frequency f for the data from (a). (c) Data from (b) averaged over the band 0.0625–3 Hz vs voltage V biasing the samples. The solid line has the slope of 2.

experimental circuit for this technique. Two V12 specimens, each of approximately equal resistance $\cong 1/2R$, were placed in the bottom arms of the Wheatstone bridge. They were biased through ballast metallic film resistors of resistance $\cong 1/2R_B (R_B \gg R)$. At room temperature the total resistance R of the pair of samples was 17.2 kΩ. The bridge was balanced and the signal taken from resistors' side contacts at the bridge diagonal was amplified. It was then demodulated in a phase-sensitive detector, low-pass filtered, and Fourier transformed to obtain power spectral density. A few words of comment are to be said concerning the choice of the carrier (excitation) frequency. It was chosen to make the products of mixing carrier frequency and harmonics of line frequency (50 Hz) as low as possible and to make their frequencies as large as possible. Since the lowest amplitudes of the line frequency harmonics were observed at 300 and 350 Hz, the carrier frequency was set in the middle of this range. After demodulation, the signal of 25 Hz appears which is the result of mixing the carrier frequency of 325 Hz and the two harmonics mentioned above. Below this frequency no disturbing frequencies were observed in the output signal.

Power spectral densities S_V were usually gathered in a frequency f range 0.0625–25 Hz for several (ac) voltages V biasing the sample. The background noise (for $V=0$) was measured as well. The spectrum $S_{V=0}$ was flat as it was the sum of thermal and instrumental noise. $S_{V=0}$ was then subtracted from S_V to give power spectral density of excess noise $S_{Vex} \equiv S_V - S_{V=0}$. The latter had $1/f$ shape so the product fS_{Vex} averaged ($\langle\rangle$) over the band 0.0625–3 Hz was used to estimate (bias dependent) noise level. The data obtained in this way were then arranged into $\log\langle fS_{Vex}\rangle$ versus $\log V$ plots. Successive steps of this procedure are illustrated in Fig. 6.

It is well-known, that if resistance fluctuations are the source of the noise, then $S_{Vex} \sim V^2$ dependence is expected. It is really observed in our experiments at low voltages. Indeed, the solid line in Fig. 6(c) has the slope of 2 and it is evident that at low voltages the experimental points follow this line. So, the relative noise intensity (noise index) defined as[8]

$$S \equiv \lim_{V \to 0} \langle fS_{Vex} \rangle / V^2, \tag{1}$$

is a voltage independent quantity. With this quantity S_{Vex}/V^2 can be written as $S_{Vex}/V^2 = S/f$. When samples are biased by a constant current (our case) it follows directly from the Ohm law that $S_{Vex}/V^2 = S_R/R^2$, so in fact, S is a measure of low-frequency resistance fluctuations. At larger voltages S_{Vex} is no longer linear with V^2, the same is valid for the dependence S_R on R^2. This may be due to either the self-heating of the samples or some intrinsic nonlinear phenomenon. Leaving this question aside for a while (Ref. 9), let us note that for the low-temperature sensor application low-voltage region is crucial. For that reason we restrict our consideration only to this domain, where the quantity defined in Eq. (1) completely determines the device characteristics.

In Fig. 7 the relative noise intensity S defined in Eq. (1) is plotted versus temperature. As it is seen in this figure below 4 K S increases significantly with decreasing tempera-

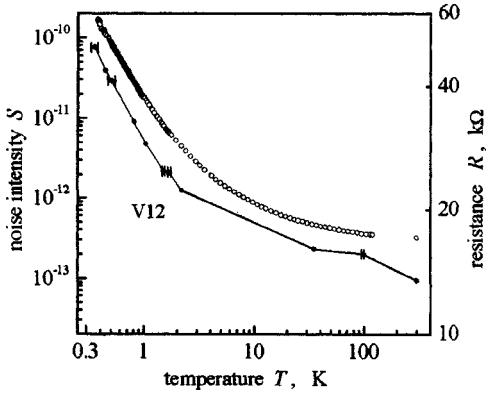

FIG. 7. Relative noise intensity S defined in Eq. (1) (left axis—dots) and resistance R (right axis—circles) vs temperature T measured for the samples V12. $R(T)$ is that of Fig. 1 plotted in log-log coordinates.

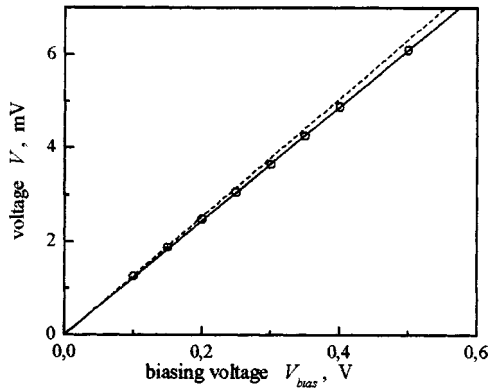

FIG. 8. Voltage V across the sample vs voltage V_{bias} biasing the bridge circuit of Fig. 5. Data are obtained at $T=0.45$ K during noise measurements.

ture approaching the value of $\sim 10^{-10}$ at ~ 0.3 K. This figure presents the main experimental results of the paper. Some comments are required concerning the error bars appearing in this figure. The uncertainties in the estimation of ambient temperature come from the self-heating of the samples, which takes place during the noise measurements. Figure 8 explains this effect in a more quantitative way. This is a plot of voltage V across the sample versus voltage V_{bias} across the whole bridge (see Fig. 5). As the upper voltage leg, on which V is measured, is in 2/3 part of the specimen V12, the resistance R can be calculated from the following relation:

$$V = \frac{R}{1.5R + R_B} V_{\text{bias}}. \tag{2}$$

It is clear from Fig. 8, that the lines drawn through the points on the graph corresponding to the lowest and the highest values of bias have different slopes. So, two different values of resistance R can be calculated, which differ by some amount. When put onto $R(T)$ characteristic (of Fig. 7) they uniquely define the change of temperature that takes place during noise measurements.

IV. RESOLUTION OF TEMPERATURE MEASUREMENT

Temperature is not a directly measurable quantity, but rather inferred from other measurements, which can be made directly. Modern instruments like, e.g., the Lake Shore Model 370 AC Resistance Bridge or Stanford Research Systems SIM921 AC Resistance Bridge use a four lead, ac measurement technique and sinusoidal current excitation for measuring the resistance. It takes advantage of the phase sensitive detection which is used in the lock-in amplifiers. The phase sensitive detector (PSD) is a very narrow band pass filter. The output of the PSD is run through an analog low pass filter to give an equivalent dc voltage. Once the dc voltage is digitized, additional digital averaging can be chosen to reduce bandwidth further and to improve the resolution. When the resistance is measured, it is then converted to temperature for calibrated resistance thermometers. Conversion is based on the temperature response curve data loaded into the instrument's memory.

The resolution $\varepsilon_T \equiv \Delta T$ of temperature measurement is limited by the measurement system resolution according to the expression[10]

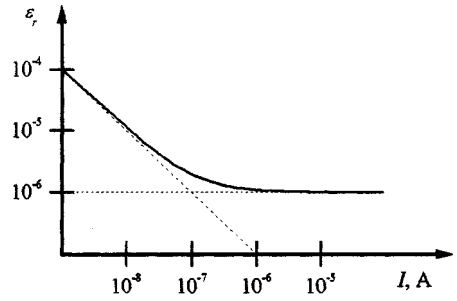

FIG. 9. Relative measurement resolution for the instrument operating with the resistance-type sensor. Solid line is the plot of Eq. (4) with $T=300$ K, $R=135$ kΩ, $\tau=3$ s, and $\varepsilon_0=10^{-6}$. Dashed lines are the plots of the first and the second terms on the right-hand side of Eq. (4).

$$\frac{\varepsilon_T}{T} = \frac{\varepsilon_r}{A}, \tag{3}$$

where A is the specific sensitivity, which for the resistance-type sensors is defined as $A \equiv d \ln R / d \ln T$ and ε_r is the measurement system relative resolution. The latter, for the instruments reading-out the sensor's resistance, is defined as $\varepsilon_r \equiv \Delta R/R$. Both Lake Shore and Stanford Research Systems define ΔR as rms noise low-pass filtered with $\tau=3$ s time constant measured on a room temperature resistor. Equation (3) states that the temperature resolution is described once the resolution of the measurement system is specified. The use of ac excitation, phase sensitive detection, proper guarding, and shielding make it now possible to achieve the instrument resolution of $\varepsilon_0=10^{-6}$ at high enough excitation currents. At low excitation, however, ε_r increases due to the (irreducible) thermal noise of the resistor. For the instruments operating at constant current mode we have

$$\varepsilon_r = \frac{\Delta R}{R} = \frac{\Delta V}{V} = \frac{V_{\text{tn}} + V_{\text{in}}}{V} = \frac{\sqrt{4kTR\Delta f}}{IR} + \varepsilon_0, \tag{4}$$

where $V_{\text{tn}}, V_{\text{in}}$ are rms voltages of thermal and instrumental noise, respectively, $\Delta f = (4\tau)^{-1}$ is the noise bandwidth of the output filter, k is Boltzmann constant. In Fig. 9 relative resolution ε_r of Eq. (4) is plotted versus excitation current for $R=135$ kΩ. Much more information is stored in Fig. 10, where relative power spectral densities S_R/R^2 of resistance fluctuations at the instrument output are plotted for several excitation currents. The measurements were performed with high-resolution Lake Shore Model 370 AC Resistance Bridge for several excitation currents. This instrument enables continuous recording of resistance with ten readings per second rate. At the excitation currents as low as $I=3.16$ nA or $I=10$ nA the spectra are flat up to the instrument cutoff frequency of $(2\pi\tau_{\text{min}})^{-1}$. For the instrument used in the experiment $\tau_{\text{min}}=0.2$ s. Such a shape of the spectra is well understood, since under the constant-current measurement conditions and at low-current limit we have

$$\frac{S_R}{R^2} = \frac{S_V(f)}{V^2} \cong \frac{4kTR}{I^2R^2} = \frac{4kT}{RI^2}. \tag{5}$$

Integration of two most upper spectra in Fig. 10 over the band Δf gives the square of the first term on the right-hand side (rhs) of Eq. (4). With increasing current the component of S_R/R^2 described by Eq. (5) gets smaller and so the spectra

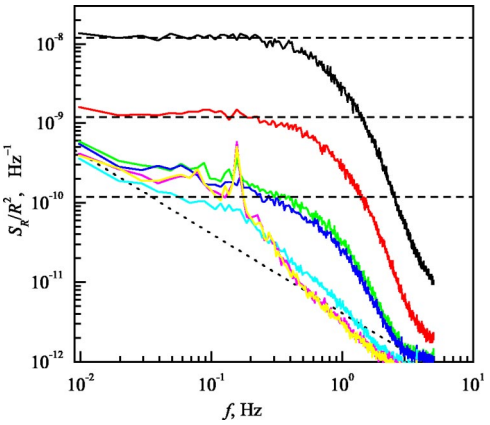

FIG. 10. (Color online) Relative power spectral densities of resistance fluctuations measured for wire-wound resistor of resistance $R=135$ kΩ at room temperature. Successive spectra from up to down are for the increasing excitation currents $I=3.16$, 10, 31.6, 100, 316 nA, 1, 3.16 μA. Dashed horizontal lines show the thermal noise limits of Eq. (5) (plots are for $I=3.16$, 10, 31.6 nA only). Dotted line is the function graph of $S_R/R^2 \cong 4.1 \times 10^{-12}/f$.

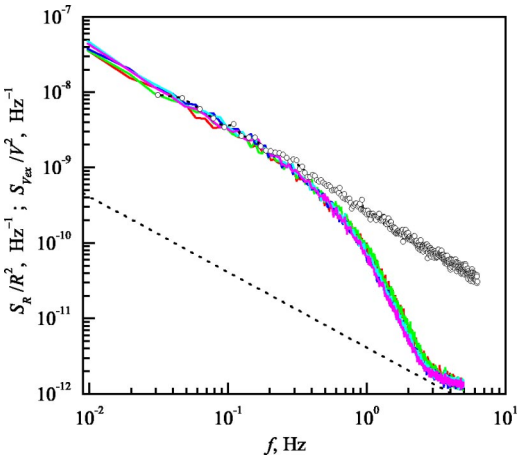

FIG. 11. (Color online) Relative power spectral densities of resistance fluctuations S_R/R^2 (solid lines) and voltage fluctuations S_{Vex}/V^2 (circles) measured on carbon WEGO resistor of resistance $R=135$ kΩ at room temperature. S_R/R^2 spectra were measured with ac resistance bridge for various excitation currents: $I=31.6$, 100, 316 nA and 1, 3.16 μA. S_{Vex}/V^2 spectrum was measured with dc current of $I_{dc}=1.6$ μA. Dotted line is the same as in Fig. 10 and shows the instrument internal noise in $f \to 0$ limit.

in Fig. 10 successively reveal the shape of instrumental noise power spectral density. The latter can be obtained at high enough currents ($I \geqslant 316$ nA) at which the spectra in Fig. 10 become almost current independent. As one can see, the specific feature of the instrument used in our experiment is the $1/f$ shape of its noise spectrum in the $f \to 0$ limit. The square root of the instrument noise spectrum integrated over the band Δf gives the value of ε_0 in Eq. (4).

Equations (4) and (5) and Figs. 9 and 10 describe the relative resistance resolution well enough only in the case, when the thermal noise is the dominating noise of the sensor. When however, the resistance noise occurs and becomes large enough, it also must be taken into account. In general, for a sensor with noise index S a new term appears in Eq. (5) and it takes the form

$$\frac{S_R}{R^2} = \frac{4kT}{RI^2} + \frac{S}{f}. \tag{6}$$

That Eq. (6) is correct, one can convince oneself looking at Fig. 11, where the measurements performed on a high-noise-level carbon resistor (WEGO) are presented. When constant dc current of $I_{dc}=1.6$ μA was passed through this resistor, the voltage fluctuations across it showed up pure $1/f$ excess noise of $S_{Vex}/V^2 \cong 2.3 \times 10^{-10}/f$ down to the lowest measurable frequency of 40 mHz (the dependence S_{Vex}/V^2 was verified). As it is shown in Fig. 11, in the $f \to 0$ limit the spectrum of S_{Vex}/V^2 overlaps with the spectra of S_R/R^2, obtained from the direct resistance measurements for several excitation currents. The overlapping seen in Fig. 11 is not surprising, since as it was shown in the previous section, the phase sensitive detection used in modern R-meters preserves resistance noise at the output signal. At the high enough currents and low enough frequencies, the second term in Eq. (6) becomes dominant, what is exactly the case seen in Fig. 11.

Taking the arguments above into account, we shall rewrite Eq. (4) in the following form:

$$\varepsilon_r = \frac{\sqrt{4kTR\Delta f}}{IR} + \varepsilon_0 + \varepsilon_{\text{sens}}, \tag{7}$$

where

$$\varepsilon_{\text{sens}} \equiv \left(\int_{1/t}^{f_\infty} \frac{S}{f} df \right)^{1/2} = [S \ln(tf_\infty)]^{1/2} \cong (2.3 \times S)^{1/2} \tag{8}$$

defines the excess noise resolution of a temperature sensor. In the expression above, t is the time of observation and f_∞ is the upper cutoff frequency of the output filter ($f_\infty = \Delta f$). In practice it is necessary to keep t at least an order of magnitude larger than the filter time constant. So, assuming $tf_\infty = 10$ seems to be a reasonable choice for the sensor characterization purposes. For instance, for our V12 sensor we thus have $\varepsilon_{\text{Ru02}} = 1.3 \times 10^{-5}$ at $T=0.36$ K. Sensitivities at other temperatures are gathered in Table I.

V. DISCUSSION

It is important to note that the resolution $\varepsilon_{\text{sens}}$ is current independent [as S in Eq. (8) is the bias independent quantity]. So, in general, it does not make sense to increase the excitation expecting to achieve better resolution. It is clearly seen in Fig. 11, where the quantity S_R/R^2 measured at several excitation currents follows (more or less) the same line as $f \to 0$. Increasing the current makes sense only until the resolution connected with thermal noise is suppressed below the resolution connected with the resistance noise. We then may write down the following condition:

$$\sqrt{\frac{4kTf_\infty}{I^2R}} \leqslant \varepsilon_{\text{sens}}, \tag{9}$$

from which the optimum current for making the measurements can be easily calculated. It also stems from Eq. (9), that the same effect can be achieved by decreasing the bandwidth f_∞ of the output filter. Nevertheless all these efforts cannot make the overall resolution lower than the limit de-

TABLE I. Sensitivities calculated for V12 sensor at various temperatures.

T, K	ε_{RuO2}
0.36	1.31×10^{-5}
0.45	9.46×10^{-6}
0.51	8.11×10^{-6}
0.8	4.55×10^{-6}
1.04	3.32×10^{-6}
1.51	2.23×10^{-6}
2.2	1.68×10^{-6}
35	7.31×10^{-7}
98	6.78×10^{-7}
300	4.69×10^{-7}

termined by Eq. (8). So we conclude that low-frequency resistance noise becomes a factor, which limits strongly the resolution of RuO_2-based thermometers at liquid helium temperatures. As it is a sensor-dependent phenomenon, we have found it proper to relate a new parameter ε_{sens} with a sensor rather than to a R-reading instrument. The overall resolution of a sensor + instrument setup is given by Eq. (7). In a more general case, when more noise sources are involved, ε_r should be estimated as direct sum of all-source resolutions in the worst-case (conservative) approach, or as the summed up squared components resolutions in (less conservative) most probable approach.[10]

At the end let us note that our experiments show that the increase of low-frequency noise of RuO_2-based temperature sensors which occurs at liquid helium temperatures results from equilibrium fluctuations of the sensor's resistance. As discussed above such noise can strongly influence the resolution of temperature measurements. On the other hand, once the type of noise is recognized, the knowledge about it can be used to optimize the sensor's performance. For example, when thinking about sensor dimensions, the well-known feature of resistance noise: $S_R/R^2 \sim (\text{volume})^{-1}$ should be taken into account.

ACKNOWLEDGMENTS

The work was supported by Project No. U-6179/DS. Lake Shore Co. is gratefully thanked for the permission to reproduce their data sheets for RX-202A sensor.

[1] A. Kolek, P. Ptak, Z. Zawislak, K. Mleczko, and A. W. Stadler, *Proceedings of the 25th International Spring Seminar on Electronics Technology*, Prague, 2002, pp. 142–146.
[2] J. G. Rhee and T. M. Chen, Solid State Technol. **21**, 59 (1978).
[3] A. Masoero, B. Morten, M. Prudenziati, and A. Stepanescu, *Proc. 10th International Conference on Noise in Physical Systems* (Akademiai Kiado, Budapest, Hungary, 1990), pp. 561–564.
[4] A. Kolek, P. Ptak, K. Mleczko, and A. Wrona, *Proceedings of the 16th International Conference Noise in Physical Systems and 1/f Fluctuations*, Gainesville, Florida (World Scientific, Singapore, 2001), pp. 713–716.
[5] M. Affronte, M. Campani, B. Morten, M. Prudenziati, and O. Laborde, J. Low Temp. Phys. **112**, 355 (1998).
[6] http://www.lakeshore.com/temp/sen/rrtd.html
[7] J. H. Scofield, Rev. Sci. Instrum. **58**, 985 (1987).
[8] In fact, the voltage $2\times V$ should be used in the denominator of Eq. (1) to calculate relative noise intensity of the pair of samples used in the measurement setup of Fig. 5. On the other hand, as $S\sim(\text{volume})^{-1}$, measurements on voltage legs of a single V12 specimen would give the value of $4\times S$. This brings us back to the definition of Eq. (1).
[9] A. Kolek, *Proceedings of NATO ARW on Advanced Experimental Methods for Noise Research in Nanoscale Devices, Brno 2003*, edited by J. Sikula and M. Levinshtein (Kluwer, Dordrecht, 2004), pp. 245–252.
[10] D. S. Holmes and S. S. Courts, Resolution and Accuracy of Cryogenic Temperature Measurements, *Temperature: Its Measurement and Control in Science and Industry* (J. F. Schooley A/P, New York, 1992), Vol. 6, pp. 1225–1230.